IOP Publishing Environ. Res. Lett. 16 (2021) 084028 https://doi.org/10.1088/1748-9326/ac12f2

ENVIRONMENTAL RESEARCH
LETTERS

OPEN ACCESS

RECEIVED
5 May 2021

REVISED
1 July 2021

ACCEPTED FOR PUBLICATION
9 July 2021

PUBLISHED
4 August 2021

LETTER

Spatial configuration and time of day impact the magnitude of urban tree canopy cooling

Michael Alonzo[1,*], Matthew E Baker[2], Yuemeng Gao[1] and Vivek Shandas[3]

[1] Department of Environmental Science, American University, Washington, DC, United States of America
[2] Department of Geography & Environmental Systems, University of Maryland, Baltimore County, Baltimore, MD, United States of America
[3] Nohad A. Toulan School of Urban Studies and Planning, Portland State University, Portland, OR, United States of America
[*] Author to whom any correspondence should be addressed.

E-mail: alonzo@american.edu

Keywords: urban heat island, urban forest, air temperature, landscape context, tree canopy

Supplementary material for this article is available online

Abstract

Tree cover is generally associated with cooler air temperatures in urban environments but the roles of canopy configuration, spatial context, and time of day are not well understood. The ability to examine spatiotemporal relationships between trees and urban climate has been hindered by lack of appropriate air temperature data and, perhaps, by overreliance on a single 'tree canopy' class, obscuring the mechanisms by which canopy cools. Here, we use >70 000 air temperature measurements collected by car throughout Washington, DC, USA in predawn (pd), afternoon (aft), and evening (eve) campaigns on a hot summer day. We subdivided tree canopy into 'soft' (over unpaved surfaces) and 'hard' (over paved surfaces) canopy classes and further partitioned soft canopy into distributed (narrow edges) and clumped patches (edges with interior cores). At each level of subdivision, we predicted air temperature anomalies using generalized additive models for each time of day. We found that the all-inclusive 'tree canopy' class cooled linearly at every time (pd = 0.5 °C ± 0.3 °C, aft = 1.8 °C ± 0.6 °C, eve = 1.7 °C ± 0.4 °C), but could be explained in the afternoon by aggregate effects of predominant hard and soft canopy cooling at low and high canopy cover, respectively. Soft canopy cooled nonlinearly in the afternoon with minimal effect until ∼40% cover but strongly (and linearly) across all cover fractions in the evening (pd = 0.7 °C ± 1.1 °C, aft = 2.0 °C ± 0.7 °C, eve = 2.9 °C ± 0.6 °C). Patches cooled at all times of day despite uneven allocation throughout the city, whereas more distributed canopy cooled in predawn and evening due to increased shading. This later finding is important for urban heat island mitigation planning since it is easier to find planting spaces for distributed trees rather than forest patches.

1. Introduction

Replacement of natural landscapes with impervious surfaces results in the urban heat island (UHI) where temperatures are higher compared to adjacent rural areas (Oke 1982). Urban heat has been implicated in a range of human health concerns (Heaviside *et al* 2017), increased stress on green and gray infrastructure, and higher greenhouse gas emissions related to climate control (Roxon *et al* 2020). There is substantial research demonstrating that areas with higher impervious surface cover and/or lower vegetation cover are hotter as assessed either by air (Wang *et al* 2017) or land surface temperature (LST; Roberts *et al* 2012). Moreover, citywide and neighborhood-scale relationships between urban three-dimensional structure and temperature (e.g. 'local climate zones'; Stewart and Oke 2012) are well established. However, understanding of fine-scale connections between urban temperature and its biophysical drivers remains limited.

Trees in urban environments cool through a combination of shading and transpiration, but the magnitude of the effect depends on the amount of canopy cover surrounding observation points (Shiflett *et al* 2017, Ziter *et al* 2019, Cao *et al* 2021). Although

some studies have shown linear relationships between canopy cover and cooling (Logan *et al* 2020), there is mounting evidence that this relationship is more often nonlinear, showing limited cooling until 25%–50% cover and becoming more substantial at higher values (Alavipanah *et al* 2015, Logan *et al* 2020, Jung *et al* 2021). However, more information is needed to understand the reasons for this nonlinearity as well as its applicability across climate zones. Furthermore, the strength of the measured relationship between canopy and cooling appears to be scale dependent (Ziter *et al* 2019) but the extent of the zone of influence is not well characterized and will likely vary with time of day.

The strength of relationship between canopy cover and temperature is partly a function of urban green typology and context. Most existing research uses broad categories to describe the distribution of urban green including remote sensing vegetation indices such as the normalized difference vegetation index (Tucker 1979) or binary urban tree canopy maps (O'Neil-Dunne *et al* 2014). Although, the latter offers more specific information regarding plant functional type and associated structural characteristics, it does not account for the spatial context of each canopy pixel. We argue in this work that both canopy position with respect to impervious surface and the extent to which canopy is clustered or distributed are important modifiers of its cooling potential. Moreover, subdividing the broad canopy class can yield a more mechanistic understanding of how canopy cools and, ultimately, can more clearly inform policy regarding effective UHI mitigation.

Closed canopy patches (i.e. large parks, woodlands), may exert strong cooling effects compared to more distributed canopy but this ecosystem service is not evenly allocated throughout most cities. The mechanisms driving cooling within and around larger patches in cities are complex and perhaps interacting. Clustered vegetation may have greater ability to cool because of higher albedo compared to distributed vegetation, thus reducing the amount of shortwave radiation absorbed at the surface (Shiflett *et al* 2017). Moreover, clustered vegetation—often found in parks, undeveloped areas, and open space—is more likely to be situated atop unpaved surfaces (hereafter, 'soft canopy') which, itself, cools due to latent heat flux of soil moisture (Gao *et al* 2020) and may also enhance vegetation function in terms of lower stress and higher and more sustained rates of transpiration (Shashua-Bar *et al* 2009, Armson *et al* 2012, Rahman *et al* 2020). This so-called *park cool island* effect (Feyisa *et al* 2014, Zipper *et al* 2016) strongly cools within the patch itself and also can cool neighboring areas some distance away (Zhou *et al* 2019) but the magnitude, distance, and direction of this effect are highly variable and dependent, for example, on wind direction and speed (Quanz *et al* 2018, Santamouris *et al* 2018).

Distributed canopy includes street and other tree plantings overhanging impervious surface (hereafter 'hard canopy') as well as soft canopy that is not part of a large patch (e.g. backyards or along linear features). Hard canopy distributed through the urban core, primarily along streets or over rooftops is thought to be beneficial for local land surface cooling from shade (Gillner *et al* 2015) as well as improvement of human thermal comfort (Armson *et al* 2012). However, the effect of hard canopy can be difficult to robustly attribute to configuration since overall canopy fractional cover is generally lower in sites proportionally dominated by hard canopy, and because tree cooling effects may be swamped by building-driven warming or cooling depending on time of day (Quanz *et al* 2018). Distributed canopy may also come in the form of scattered soft canopy such as backyard or park plantings, though minimal research has been dedicated to differentiating the cooling potential of clumped versus distributed soft canopy (Santamouris *et al* 2018). An understanding of the cooling potential of distributed canopy is important because the availability of planting spaces in cities is more likely to be scattered than either contiguous or extensive.

The relationship between urban land cover and temperature is further complicated by variability attributable to time of day. Vegetation neither shades nor transpires at night and it is still an open question whether trees or other green infrastructure offer cooling benefits after dark (Zhou *et al* 2019). On one hand, trees may trap longwave radiation (Gillner *et al* 2015) and the presence of soil moisture may increase unpaved surface thermal inertia, both contributing to a relative warming effect (Yao *et al* 2017). On the other, areas with high tree cover will have received less solar radiation at the surface throughout the day and unpaved surface may exhibit a net cooling effect, particularly under conditions of high evaporative demand (Shiflett *et al* 2017, Voelkel and Shandas 2017, Logan *et al* 2020, Ibsen *et al* 2021). During the hottest hours of the day, cooling from vegetation is critical for human thermal comfort and may be strong in locations with high cover (Ziter *et al* 2019, Cao *et al* 2021, Jung *et al* 2021). However, limitations on this ecosystem service due to midday stomatal downregulation (Gillner *et al* 2015) as well as low solar zenith angles leading to limited structural shading (Yu *et al* 2020a) merit further exploration. By contrast, evening hours could be associated with enhanced cooling due to higher solar zenith angles and reduced stomatal regulation but there has been minimal data collected in support of these hypotheses.

Research over the past decade has produced substantial insight into zonal and fine-scale processes underlying the UHI. Still, most studies are logistically hampered by the ability to sample air temperature both densely and across a meaningful extent such as a large city. *In situ* sensor networks offer

unparalleled description of city temperature temporal dynamics but are more sparsely distributed (but see Zipper *et al* 2016, Cao *et al* 2021). Satellite-based LST measurements yield a dataset that is spatially complete but suffers from issues of coarse spatial resolution (e.g. MODIS; Alavipanah *et al* 2015), infrequent revisit (e.g. Landsat; Melaas *et al* 2013), and fundamental mismatch with ecological processes and human thermal comfort (Shandas *et al* 2019). Mobile air temperature sampling offers a means to characterize large areas within a city either repeatedly (Ziter *et al* 2019) or intensively for a single day (Shandas *et al* 2019). This sampling method increases spatial data coverage by an order of magnitude or more over fixed sensors which is important for assessing the subtle interactions among urban vegetation, abiotic structures, and air temperature. To address gaps in our understanding of how vegetation modifies air temperature, we sought to disentangle the effects of tree canopy cover, configuration, and spatial context. This study addresses these questions at multiple times of day (predawn, afternoon, evening) within a large, humid subtropical city. Specifically, we ask:

(a) How does urban tree canopy modify summertime air temperature and how do those effects vary by configuration, scale of analysis, and time of day?
(b) What are the relative contributions to temperature modification by hard canopy, soft canopy, and impervious surface?
(c) Is it more effective to cool a city using large forest patches (e.g. parks) or evenly distributed canopy?

2. Materials and methods

2.1. Study site

The District of Columbia (Washington DC) has a population of 705 749 living within an area of 158 km^2 (U.S. Census 2019). DC's climate is considered humid subtropical (Beck *et al* 2018) with an August ten year average high temperature of 31 °C and low average of 22 °C. Precipitation totals 98 cm yr^{-1}, evenly spread across months with August averaging 8.7 cm (NOAA 2021). Citywide average tree canopy cover is approximately 38% but unevenly distributed, in part because 19% of DC is parkland (figure 1(b); TPL 2011). The urban forest is almost entirely broadleaf deciduous with common species including American Beech and Red Maple in natural and managed landscapes, respectively (Casey Trees 2015). Impervious surface covers 39% of the city, unevenly as much of the area outside of downtown is populated by single family row or separated homes. Building heights in the downtown core are less variable than many cities due to a height restriction requiring that buildings be roughly as tall as their fronting street is wide (~40 m).

2.2. Data description

Mobile and station air temperature data as well as additional station meteorological data were collected on 28 August, 2018. August 28 was selected as a useful case study because it was hotter (min = 25 °C, max = 35 °C) than DC's August average temperatures thus highlighting the distribution of urban heat under warming conditions. Additionally, conditions were fair: clear to partly cloudy skies with low wind and no precipitation during the sampling period or anytime in the previous week. These conditions are typical of a DC summer day and also minimize concerns that spatial variability in temperature data was driven by advection or standing water. The mobile air temperature data and collection methods are presented fully in Shandas *et al* (2019). Briefly, nine cars were outfitted with temperature sensors (type 'T' thermocouple with radiation shield mounted 25 cm above car roofs, as illustrated in Voelkel and Shandas (2017), to minimize heat interference from car exhaust) coupled with Global Positioning System (GPS) to record position and velocity. Data were collected at 1 s intervals three times during the day: from 5:00 to 6:00 ('predawn'), 14:00 to 15:00 ('afternoon') and 18:00 to 19:00 ('evening'). Collection periods, selected to sample minimum and maximum heat ('predawn', 'afternoon') as well as a transition period with high structural shading ('evening'), were kept to 1 h to minimize impacts of changing weather throughout the day. Sunrise and sunset were at 6:33 and 19:45 respectively. To further minimize the effect of mesoscale meteorological variability, we subtracted weather station air temperature—recorded at 5 min intervals—from the mobile temperature readings. The station temperature was computed as the average of four downtown DC weather stations with high site similarity in terms of low canopy cover and high imperviousness (figure 1; Ziter *et al* 2019) resulting in mobile anomaly temperature distributions with a mean below zero. Wind speed, wind direction, and downwelling shortwave radiation data were recorded at only one downtown station. Wind speed and direction are highly localized at street level and thus we prioritized acquisition of sensible, citywide data (i.e. no averaging of wind direction measurements) over minor improvements in representativeness. Finally, to reduce potential effects from anthropogenic sources (e.g. vehicle and building exhaust) the raw temperature data were further processed to remove measurements occurring when vehicle speeds were below 15 km h^{-1}.

Geospatial predictor variables were produced using freely available planimetric and lidar data from the City of Washington, DC data repository (table 1). We produced a high-resolution urban tree canopy map of the city using lidar collected in April 2019 (partial leaf off). The canopy map, evaluated at 327 validation points, yielded a citywide canopy cover

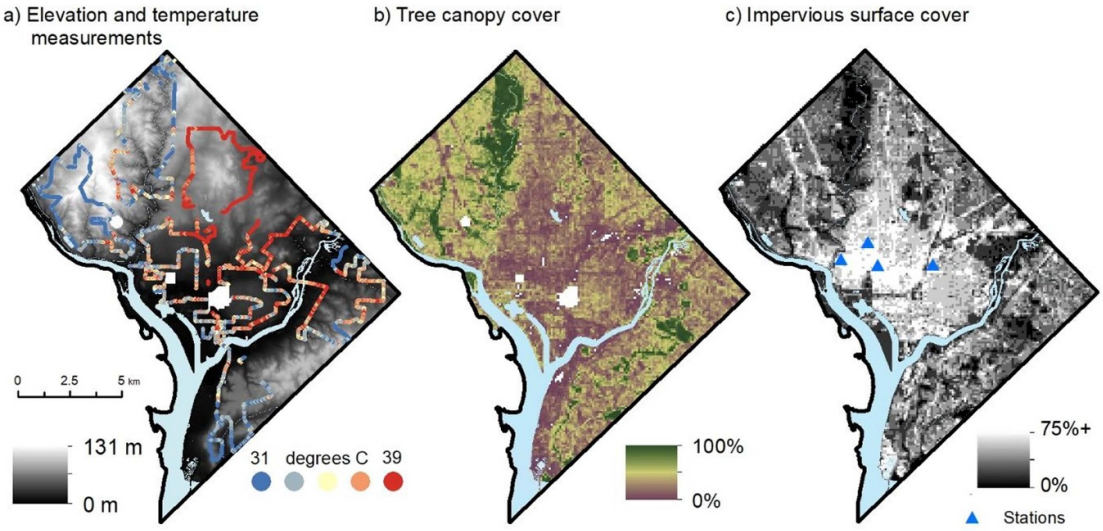

Figure 1. Washington, DC study area: (a) elevation with car routes overlaid. Temperatures are from afternoon collection ranging between 31 °C and 39 °C. Missing data (white patches) are in restricted zones (e.g. US Capitol). (b) Tree canopy cover percent in 100 m pixels. (c) Impervious surface cover percent in 100 m pixels This panel also shows the location of our four reference weather stations.

Table 1. Data descriptions.

Variable name	Short name	Description
Vegetation		
Tree canopy	TCF	1 m tree canopy map derived from 2018 City of DC lidar data
Soft canopy	SCF	Tree canopy that does not overhang impervious surface
Hard canopy	HCF	Tree canopy that overhangs impervious surface
Canopy patches	PATCH	Soft canopy patches large enough to have cores (MSPA)
Distributed canopy	DISTRB	Soft canopy, connected or unconnected, no core (MSPA)
Pervious-open	PV-O	Area that is neither soft canopy nor impervious surface
Built environment		
Impervious surface	IMP	Impervious surface from City of DC planimetric data
Building height (sum)	BH	Building heights summed in area (DC building footprints and lidar data)
Building height (IMP norm)	BH-norm	Building heights as above but normalized by IMP to decorrelate
Skyview factor	SVF	Skyview factor calculated using DC lidar data in SAGA GIS
Physiographic		
Elevation	ELEV	City of DC lidar Digital Terrain Model (2018)
Quantile elevation	Q-ELEV	Quantile (local) elevation within 300 m radius
Distance from water	DIST-W	Euclidean distance from Potomac and Anacostia rivers
Car data		
Spatial coordinates	LON, LAT	Temperature measurement locations geographic coordinates
Mobile temperature	MBL-T	Temperature measurements (celsius)
Miles per hour	MPH	Car travel speed
Station data		
Station temperature	ST-T	Temperature (celsius) averaged across four downtown DC stations
Station wind speed	ST-WS	Wind speed at one representative station
Station wind direction	ST-WD	Wind direction at one representative station
Station solar radiation	ST-SR	Solar radiation at one representative station

estimate of 38.2% compared to 38.2% estimated directly from aerial images (0% quantity disagreement indicating lack of model bias). When accounting for the specific location of canopy at 1 m resolution, the overall accuracy of the canopy map was 91%. Impervious surface cover was taken directly from the city planimetric layer as were building footprints. Skyview factor was calculated as the fraction of visible sky from each temperature measurement point based on the city's digital surface model. Hard canopy was determined by its overlap with impervious surfaces including rooftops, roads, and other paved surfaces. Patches of soft canopy were distinguished from distributed canopy using morphological spatial pattern analysis (MSPA; Vogt *et al* 2007) using an edge parameter of 15 m based on observed

changes in vegetation composition and structure (Baker, *unpublished* data). MSPA applies the edge parameter to distinguish interiors (i.e. 'cores') from surrounding edges, as well as five other morphometric primitives (i.e. branches, bridges, loops, and islets) that reflect how canopy is or is not connected to cores. 'Patches' always included core areas, their surrounding edges, as well as any perforations, whereas 'distributed' canopy included all remaining non-patch MSPA classes too small to contain core. To understand the scales of interaction between biophysical variables and anomaly temperature, all variables were summarized at each temperature point within buffers ranging from 10 to 800 m (Ziter *et al* 2019).

2.3. Analysis using generalized additive models (GAMs)

The relationship between some biophysical variables—most notably tree canopy cover—and air or LST can be nonlinear in nature (Ziter *et al* 2019, Logan *et al* 2020). GAMs are a nonparametric technique that can fit smooth curves between predictor and response variables using penalized regression splines (Pedersen *et al* 2019). In this study, we used the *gam* function in the R package 'mgcv' (version 1.8.31) and fit the models using fast restricted maximum likelihood.

We employed three models to address our research questions regarding the importance of the quantity and spatial configuration of tree canopy and other unpaved surfaces. Model #1 (M1) establishes continuity with previous work and compares the relative effects of all tree canopy cover and impervious surface on temperature (Ziter *et al* 2019). Model #2 (M2) is formulated with the purpose of disentangling the cooling effects of soft canopy, hard canopy, and impervious surface. Model #3 (M3) further subdivides soft canopy in order to establish the relative cooling effects of large canopy patches (e.g. parks) versus distributed canopy (e.g. backyard planting). The three models are formulated as:

$$\begin{aligned}(\mathrm{M1})\quad T_{\mathrm{anom}} \sim\ & s(\mathrm{TCF}) + s(\mathrm{IMP}) + ti(\mathrm{TCF}, \mathrm{IMP}) \\ & + s(\mathrm{ELEV}) + s(\mathrm{ST}-\mathrm{WS},\ \mathrm{by} = \mathrm{ST}-\mathrm{WD}) \\ & + s(\mathrm{LON},\ \mathrm{LAT})\end{aligned}$$

$$\begin{aligned}(\mathrm{M2})\quad T_{\mathrm{anom}} \sim\ & s(\mathrm{SCF}) + s(\mathrm{HCF}) + s(\mathrm{IMP}) \\ & + ti(\mathrm{SCF}, \mathrm{IMP}) + s(\mathrm{ELEV}) \\ & + s(\mathrm{ST}-\mathrm{WS}, \mathrm{by} = \mathrm{ST}-\mathrm{WD}) \\ & + s(\mathrm{LON},\ \mathrm{LAT})\end{aligned}$$

$$\begin{aligned}(\mathrm{M3})\quad T_{\mathrm{anom}} \sim\ & s(\mathrm{PATCH}) + s(\mathrm{DISTRB}) + s(\mathrm{HCF}) \\ & + s(\mathrm{IMP}) + ti(\mathrm{PATCH}, \mathrm{IMP}) + s(\mathrm{ELEV}) \\ & + s(\mathrm{ST}-\mathrm{WS}, \mathrm{by} = \mathrm{ST}-\mathrm{WD}) \\ & + s(\mathrm{LON},\ \mathrm{LAT}).\end{aligned}$$

Variable descriptions are available in table 1. The *s*() notation indicates that the response is assumed to be a smoothed function of the predictor, facilitating the method's accommodation of nonlinearity. The *ti*() houses an interaction term that additionally has main effects included in the model. Canopy variables were included in the model based on the core research questions and were thus not subject to scrutiny in terms of their model utility as assessed using Akaike's information criterion (AIC). Interaction terms and non-canopy variables, however, were included on the basis of lowering AIC compared to alternative models. Thus, each model accounts for any significant interactions between impervious surface and a canopy variable as well as elevation, wind speed, and wind direction. Other variables that have been significant in previous studies including distance from water (Ziter *et al* 2019) and those related to building heights or urban canyon configurations (Voelkel and Shandas 2017) did not merit inclusion in our models. Spatial coordinates were included to account for residual model spatial structure in the T_{anom} that was not explained by our biophysical predictor variables. Spatial autocorrelation was reduced through systematic subsampling of the data, which consisted of fitting a model using 5% iteratively 20 times resulting in an approximate spacing of 100 m between nearest measurement points. Nevertheless, given that spatial autocorrelation is likely not entirely eliminated and GAMs can overestimate the nonlinearity of functional relationships in its presence, we restricted the maximum degrees of freedom to three basis functions per smooth term and nine for interactions (Wood 2017). The spatial term was allowed 27 basis functions to flexibly fit to location-specific temperature anomalies not accounted for through functional relationships. We report mean and variability across 20 model fits as well as average estimated degrees of freedom (edf).

3. Results

3.1. Spatial scale of analysis

Prior to producing parameter estimates for the GAM smooth and interaction terms by model, we established a reasonable spatial unit for these analyses using M2 only (under the assumption that the spatial scale of cooling by canopy would be consistent across models). We iterated through the model at buffer radii of 10, 30, 90, 200, 300, 500, and 800 m at each time of day (predawn, afternoon, evening). Using fraction of variance explained (R^2) as our metric for model fit, we generally found that the models explained the highest proportion of variance in the predawn, followed by evening, and then afternoon (figure 2(a)). Maximum *R*-squared values were found at 500, 90, and 200 m for predawn, afternoon, and evening periods respectively highlighting local

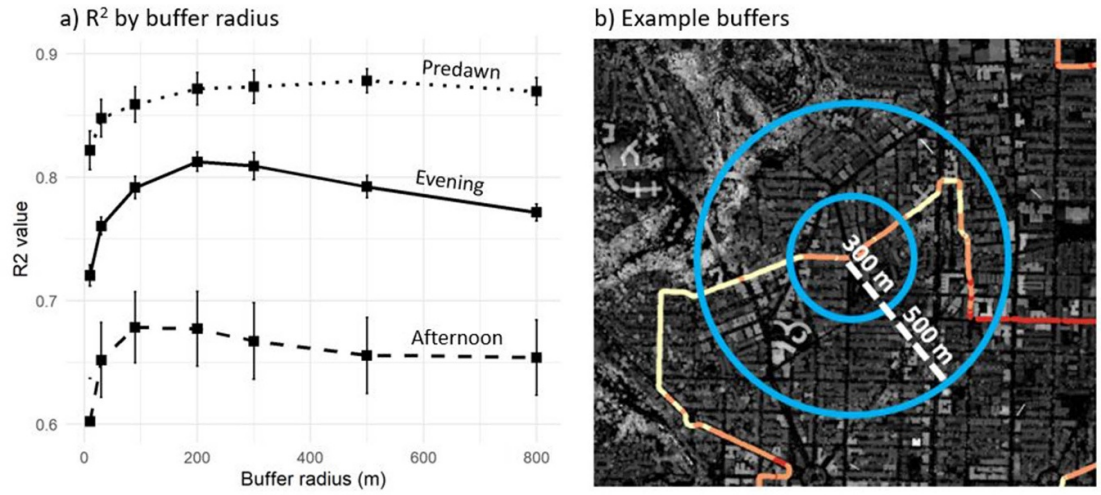

Figure 2. (a) The relationship between buffer size and model fit for predawn (5:00–6:00), afternoon (14:00–15:00), and evening (18:00–19:00) time periods. Error bars here and in all other figures are the 95% CI of the mean based on 20 iterations of systematically subsampled locations. (b) Example 300 and 800 m buffers centered on a relatively warm set of temperature measurements and overlaid on a lidar canopy height model.

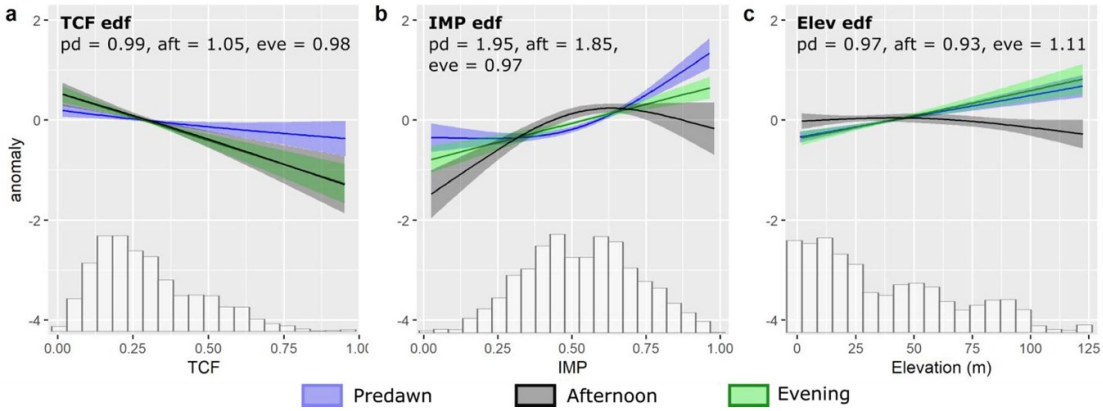

Figure 3. Model 1 results at 200 m scale by time of day where blue is predawn, black is afternoon, and green is evening. Data distributions accompany below. Estimated degrees of freedom (edf) average of 20 iterations. (a) Tree canopy fraction (TCF) cooling; (b) warming from impervious surface fraction (IMP); (c) temperature change driven by elevation.

scale effects such as shading during the afternoon and greater, near-zonal scale stability in the predawn hour. By 800 m distant from the measured temperature, it is likely that the biophysical variable summaries are combining information from multiple, distinct land uses in a manner that does not strongly relate to the measured temperature at that point (e.g. natural forested area included in 800 m buffer but not likely influencing this area of relatively warm temperatures; figure 2(b)). For consistency in presenting this work, all further analyses were conducted at the 200 m spatial scale as the differences in R^2 values between 90 and 200 m (afternoon) and 200 and 500 m (predawn) were quite small.

3.2. Tree canopy and impervious surface (M1)

In the hottest part of the day (afternoon), tree canopy exerted a linear cooling effect of 1.8 °C (figure 3(a); between 5% and 90% cover). At the same time, the warming effect from impervious surface was 1.3 °C (across the same range of cover) but convex nonlinear in shape (figure 3(b)). More rapid warming was evidenced at low cover fractions with minimal warming at high fractions, perhaps highlighting the cooling effect from building shade in the downtown area. The interaction between tree canopy and impervious surface was an important driver of cooling of up to 1.6 °C but only at high tree canopy fraction (TCF) (>0.6) and low impervious surface fraction (IMP) (<0.2) (figure S1 (available online at stacks.iop.org/ERL/16/084028/mmedia)). Evening cooling from TCF changed little from afternoon (1.7 °C) but heating from impervious surface (1.4 °C) became more linear as building shading and longwave trapping began to counterbalance. In predawn, TCF exhibited small cooling effect (0.5 °C) and impervious surface warming (1.6 °C) once again became nonlinear but concave in shape highlighting the nighttime effect of longwave

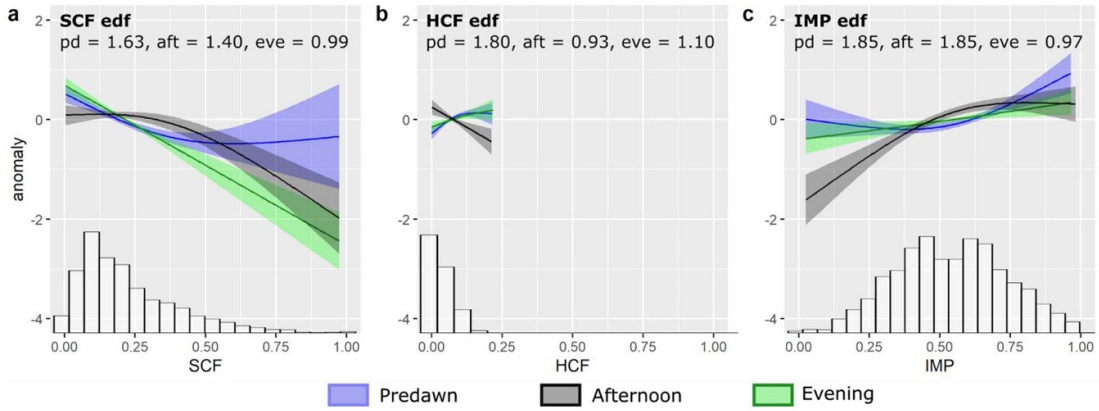

Figure 4. Model 2 results at 200 m scale by time of day where blue is predawn, black is afternoon, and green is evening. Data distributions accompany below. Effects from: (a) soft canopy fraction (SCF); (b) hard canopy fraction (HCF); (c) impervious surface fraction (IMP).

trapping in the most built-up areas. Elevation had minimal effect on temperature in the afternoon, but lower elevation areas were approximately 1 °C cooler than their surroundings in the evening and predawn due to cold air pooling in local depressions and valleys (figure 3(c)). The elevation effect was consistent across models and thus will not be reported further.

3.3. Green space partitioning: soft canopy, hard canopy, and impervious surface (M2)

Soft canopy fraction (SCF) cools at all times of day but the magnitude of the effect as well as the shape of best fit changes. In the afternoon, SCF exerts minimal cooling until ∼40% cover after which the effect strengthens with total cooling of 2.0 °C (figure 4(a)). In the evening, SCF cools very effectively (2.9 °C) and linearly across the full range of values. Contrary to some previous reports, SCF also cooled modestly in the predawn hours (0.7 °C) albeit with high uncertainty at higher cover fractions likely due to unaccounted for spatial structure and sparse data. Hard canopy fraction (HCF) had a smaller overall influence on temperature, though cover never exceeded 20% given that much HCF occurred in tree wells along streets. Nevertheless, in the afternoon, HCF cooled 0.2 °C between 0% and 25% cover compared to 0.0 °C SCF cooling across the same cover range (figure 4(b)). HCF in the evening and predawn hours was associated with a small amount of warming. The interaction between SCF and IMP was similar though less prominent in the afternoon in M2 compared to M1, at maximum accounting for 1.0 °C of cooling at the highest SCF cover and lowest impervious fraction (figure S1). Impervious surface cover (main effect) and elevation played very similar roles at each time of day in this model as in M1.

3.4. Soft canopy partitioning: patches versus distributed

We found that large patches with core (PATCH) and distributed soft canopy (DISTRB) each produced significant cooling effects, but their relative efficacies depended on time of day. In the predawn hours, incremental additions of DISTRB offered the most cooling per unit canopy cover at low cover: ∼0.8 °C from 0% to 25% cover compared to only ∼0.3 °C for PATCH, but patches continued cooling linearly from 25% to 50% cover (figure 5(b)). Areas with the lowest DISTRB cover have even less canopy cover than the downtown reference stations (19.5% cover within 200 m) potentially explaining the ∼0.7 °C positive anomaly at the predawn intercept. In the afternoon, DISTRB did not contribute to cooling (figure 5(c)). Instead, PATCH provided the bulk of the cooling effect to 50% cover (1.0 °C) with the PATCH-IMP interaction moderately important at the highest cover fractions and lowest impervious cover (0.5 °C; figure S1). In the evening, both configurations cooled strongly and roughly linearly to 50% cover (PATCH = 1.8 °C, DISTRB = 1.4 °C). To address the spatial distribution of the cooling by canopy configuration we mapped PATCH and DISTRB showing that there are many more measurement locations with >10% DISTRB cover than there are for PATCH cover (figures 5(a) and 6). This suggests that DISTRB may be offering cooling services across a broader area to a much greater percentage of the city population.

4. Discussion

We found that, on our single measurement day, between 5% and 95% cover, overall tree canopy (TCF) related to approximately 1.8 °C of afternoon cooling, which is more than the ∼1 °C effect reported by Ziter *et al* (2019) under somewhat cooler climatic conditions and in a smaller city. Our TCF cooling effect was apparently linear at all times of day, in contrast to other studies showing a threshold effect whereby 25%–50% canopy cover was required for substantial cooling (Ziter *et al* 2019, Yu *et al* 2020b,

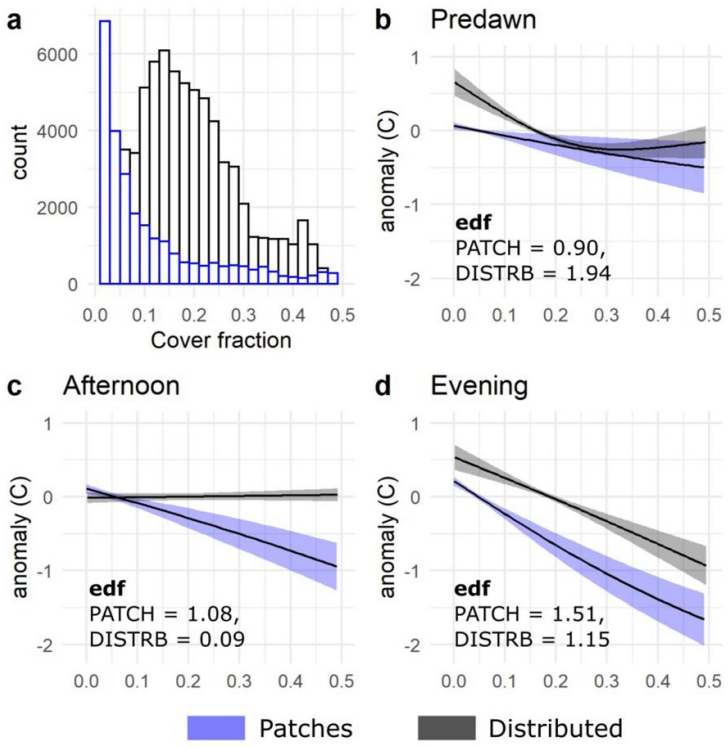

Figure 5. Disentangling the effect of soft canopy fraction on anomaly temperature into large patches (PATCH) with core and distributed soft canopy (DISTRB) with no core. Note that *x*-axis only goes to 0.5 fractional cover to account for common conditions in Washington, DC.

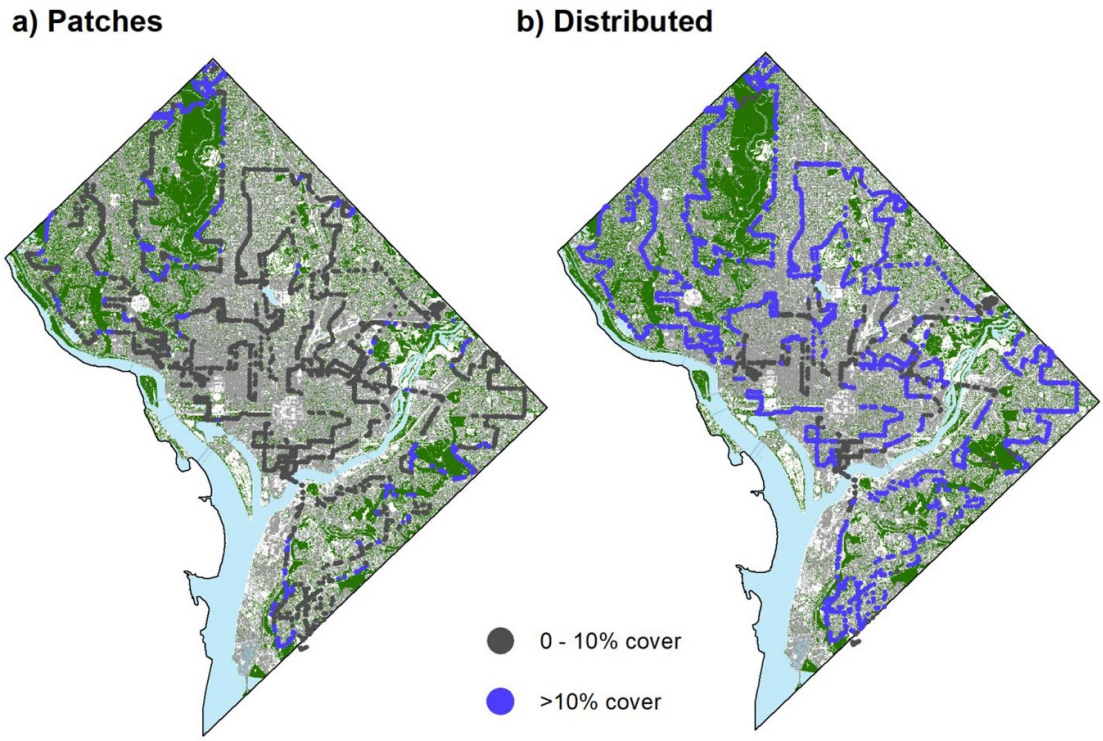

Figure 6. Distribution of (a) PATCH and (b) DISTRB throughout Washington, DC based on 200 m buffers from ∼25 000 measurement locations (5% of measurement locations displayed for clarity). Maps show where cover of each soft canopy type is >10%. Base layers are tree canopy (green), impervious surface (gray), and water (light blue). All other cover types (e.g. grass, bare soil) shown in white.

Jung *et al* 2021). The linearity observed in our study appeared to arise from combinations of HCF cooling at low cover fractions and SCF at higher cover. We suggest that findings using aggregate TCF alone may be somewhat confounded by including trees with different (HCF, SCF) growth contexts.

Partitioning overall TCF into hard and soft canopy components highlighted this importance of planting context. Soft canopy from 5% to 95% contributed slightly more to afternoon cooling compared to TCF (2.0 °C compared to 1.8 °C). Experimental work has shown that cooling is maximized in the case where tree canopy shaded grass compared to tree shade alone or grass alone (Shashua-Bar *et al* 2009) highlighting a synergistic, or at least additive, effect of multilayered vegetation. Similarly, Rahman *et al* (2020), in a review of tree traits for cooling urban areas, noted generally higher transpiration rates for trees planted over grass compared to those in 'paved cut-out pits'. While hard canopy has been shown to cool surfaces and improve urban thermal comfort, its effect on air temperature has been more limited (Armson *et al* 2012, Gillner *et al* 2015). In our study area given the lack of a buildings term in our model, it is also possible that some afternoon cooling associated with HCF is actually from building shade (Voelkel and Shandas 2017, Quanz *et al* 2018).

We found that the apparent nonlinear cooling of SCF may result from the combination of different soft canopy configurations. In the afternoon, forest patches cooled linearly to 50% cover and beyond but distributed canopy had virtually no effect on temperature (figure 5(c)). Given that distributed canopy was much more prevalent within 200 m of our sampling locations (figures 5(a) and 6), its 'no effect' signal dominated the low SCF cover signal as well. Our finding aligns with observations that the cooling effect of smaller green spaces is less consistent than that of larger parks or forests (Santamouris *et al* 2018). However, existing research has not explored how time of day factors into such apparent variability (discussed below). In Washington, DC, there were no observations of distributed canopy above 50% cover, so SCF cooling was driven entirely by those few locations within 200 m of large patches (figure 6). Large forest patches, therefore, have a unique capacity to sustain a cooling effect in the heat of the afternoon when scattered soft canopy cannot. This is consistent with recent findings emphasizing the importance of the larger size patches, higher leaf area (multilayered vegetation), and higher albedo for stable cooling in high heat (Hardin and Jensen 2007, Huang *et al* 2008, Kong *et al* 2014, Santamouris *et al* 2018, Shiflett *et al* 2017, Yu *et al* 2020b).

Zhou *et al* (2019) report in a review that 'it remains controversial' whether vegetation drives cooling during summer nights. In our study, we found soft canopy was associated with a 0.8 °C cooling effect and hard canopy was associated with a small amount of warming (0.4 °C to 25% cover) even in predawn hours. Thus, cooling in soft canopy areas at night is partially a function of perviousness, but may also leverage drivers perhaps relating to reduced daytime shortwave absorption via higher albedo or shading (Shiflett *et al* 2017). Our findings here were consistent with those of Logan *et al* (2020) who found cooling of up to 6 °C at night (using LST). Interestingly, we show that predawn cooling started at lower levels of canopy cover (figure 4(a)) and thus seemed to be driven more by distributed soft canopy than by larger patches (figure 5(b)). Thus, the apparent effect of distributed soft canopy supports the interpretation that higher cover or patch-dominated areas had either avoided heating in the afternoon or had already cooled substantially through the previous evening and night. Finally, in agreement with Acero *et al* (2013), it was important in our study area to account for local relief, particularly at night. While cold air drainage has limited bearing on vegetation function, it played a large role in the overall spatial distribution of the DC's UHI and should be considered in heat mitigation planning.

Evening (18:00–19:00) measurements highlighted strong cooling by soft canopy as well as perhaps a transition in the warming and cooling mechanisms within the urban landscape. SCF, across its range of values, cooled linearly by 3.1 °C in the evening. The linearity can be explained as efficient cooling by both patches and distributed canopy at this time of day (figure 5(d)). In our study, a 15 m tree would cast a 14 m shadow in the afternoon but shadowing would increase fourfold to 56 m in the evening. This is noteworthy because distributed trees, by definition, provide more urban shade per unit canopy than forest patches, thus highlighting their contribution to cooling during times of lower sun angle (Yu *et al* 2020a). Furthermore, radiant flux density (W m^{-2}) on the surface as a function of solar zenith angle was 2.8× higher in the afternoon than later in the evening. Higher rates of evening transpiration due to midday stomatal downregulation (Gillner *et al* 2015), suggests the potential, in vegetated zones, for the evening surface energy balance to be increasingly dominated by latent heat flux. Higher afternoon heat loads may also contribute to effective shutdown of DISTRB cooling in hot areas, whereas cooling in PATCH canopy, buffered from impervious heat loads, is maintained. While canopy cooling was substantial in the evening measurement window, effects of three-dimensional structures captured by building height and skyview variables, shown elsewhere to relate to diurnal patterns of the UHI (Voelkel and Shandas 2017, Shandas *et al* 2019), were not fully examined in this study due to limited variation from building height restrictions in Washington, DC.

Although our study robustly demonstrates the importance of soft canopy for cooling and shows the utility of mobile temperature collection for UHI

inquiry, it is not without limitation. Data collection via vehicular traverse was an effective way to sample temperature intensively throughout the city for snapshots of a representative, summer day. However, given the coordination of nine cars driven by volunteers (Shandas *et al* 2019), it is infeasible to collect repeated, coincident measurements. In sampling a substantially smaller area, Ziter *et al* (2019) did bike each traverse a minimum of three times in order to characterize the variability due to mesoscale weather conditions. Future research might also examine whether scales of interaction between the built environment and temperature remain consistent in different bioclimatic regions. The present study found that ∼200 m buffers adequately summarized the area of influence on temperature readings, but it is possible for that to vary under different advective conditions (Alavipanah *et al* 2015) or as the thermometer moves off of roadways. Regarding our understanding of the drivers of cooling: high predictor variable correlation, concurvity, and residual spatial autocorrelation add uncertainty to our results and commonly goes un- or under-reported in other studies. For instance, in Washington, DC the inverse Pearson's correlation between TCF and IMP and SCF and IMP were $r = -0.73$ and -0.81 respectively. Such correlations would likely be similar in many cities developed from a forested matrix within a temperate or humid subtropical biome. It is not possible to fully remove variable intercorrelation in an observational setup (Dormann *et al* 2013), thus, we recommend that future effort—albeit at necessarily reduced spatial extents—is dedicated to controlled experimental setups such as that of Shashua-Bar *et al* (2009).

Our findings offer insight for developing tree planting policies in urban areas. The results underscore the importance of considering locations of greatest need alongside efficient mitigation strategies. Previous studies have found that cooling is most dramatic in areas where there is already plentiful urban green (Alavipanah *et al* 2015, Ziter *et al* 2019, Jung *et al* 2021). Our model results derived from soft canopy in the afternoon align with these findings. However, the fact that substantial distributed soft canopy can support cooling at other times of day is relevant new information from a mitigation standpoint. For instance, it lends empirical support to tree planting programs that distribute trees for residents to plant in their yards, a pragmatic way to locate available planting sites (e.g. Washington, DC Department of Energy and Environment RiverSmart program; https://doee.dcgov/riversmartrebates). Still, this strategy is only viable where single-family homes are common, leaving higher intensity land uses and, sometimes, vulnerable populations underserved (figure 6). Although Jung *et al* (2021) show temperature benefits of planting in higher intensity land-uses, further research on this topic is required, as incremental removal of impervious surfaces may be the most efficacious cooling strategy for these areas.

5. Conclusion

By spatially subdividing urban tree canopy into hard versus soft contexts, distinguishing patch versus distributed configurations, and assessing their effects during predawn, afternoon, and evening hours, we found that the capacity for tree canopy to cool the surrounding environment varies substantially based on context, configuration, and time of day. Contrary to some recent studies (e.g. Alavipanah *et al* 2015, Ziter *et al* 2019), these results suggest that the all-inclusive tree canopy class (TCF) cooled linearly at all times of day, yet soft canopy (SCF) cooled nonlinearly in the afternoon, possibly indicating that the TCF class in previous studies was largely SCF. It is likely that observed linearity in TCF cooling in our study resulted from a combination of hard canopy (HCF) cooling at low cover and high cover cooling from SCF. Time of day played an important role in determining the relative cooling or warming effects from SCF, HCF, and impervious surface. In the afternoon, only HCF cooled at low cover fractions. Unlike earlier work, removal of impervious surface from highly paved areas did not result in significant cooling. This could be because the locations with the highest impervious cover also had the largest buildings, resulting in an offsetting shading effect. In the evening, SCF cooled strongly across all cover fractions while impervious surface cover warmed only slightly, but linearly. This reflects transitions in the mechanisms for canopy cooling and impervious surface warming respectively: at this time of day canopy can cool through both shading and transpiration while areas with high building density are shifting from shading to heat trapping.

We found that nonlinearity in afternoon SCF cooling was consistent with the combined effect of negligible cooling from distributed canopy and sustained cooling from patches. This highlights the unique capacity for patches to maintain function under high heat load due, perhaps, to better access to water. Importantly though, distributed canopy cooled strongly in the evening hour likely, in part, due to widespread shading, and also offered a modest cooling benefit in the predawn hours. As distributed canopy is more broadly accessible to the residents of most cities, distinguishing its effects provides useful information for UHI mitigation planning. As high resolution urban spatial datasets become more available, it will be important to test how canopy context and configuration impact cooling in cities across a variety of climate zones and development stages.

Data availability statement

The data that support the findings of this study are available upon reasonable request from the authors.

Acknowledgments

This material is based upon work supported by the National Science Foundation under Grant No. 1951647.

ORCID iDs

Michael Alonzo https://orcid.org/0000-0001-9409-2740
Matthew E Baker https://orcid.org/0000-0001-5069-0204

References

Acero J A, Arrizabalaga J, Kupski S and Katzschner L 2013 Deriving an urban climate map in coastal areas with complex terrain in the Basque Country (Spain) *Urban Clim.* **4** 35–60

Alavipanah S, Wegmann M, Qureshi S, Weng Q and Koellner T 2015 The role of vegetation in mitigating urban land surface temperatures: a case study of Munich, Germany during the warm season *Sustainability* **7** 4689–706

Armson D, Stringer P and Ennos A R 2012 The effect of tree shade and grass on surface and globe temperatures in an urban area *Urban For. Urban Greening* **11** 245–55

Beck H E, Zimmermann N E, McVicar T R, Vergopolan N, Berg A and Wood E F 2018 Present and future Köppen-Geiger climate classification maps at 1-km resolution *Sci. Data* **5** 1–12

Cao J, Zhou W, Zheng Z, Ren T and Wang W 2021 Within-city spatial and temporal heterogeneity of air temperature and its relationship with land surface temperature *Landsc. Urban Plan.* **206** 103979

Casey Trees 2015 *i-Tree Ecosystem Analysis* (Washington, DC) (available at: https://caseytrees.org/wp-content/uploads/2017/03/iTree-2015-Report_English.pdf) (Accessed 15 June 2021)

Dormann C F *et al* 2013 Collinearity: a review of methods to deal with it and a simulation study evaluating their performance *Ecography* **36** 27–46

Feyisa G L, Dons K and Meilby H 2014 Efficiency of parks in mitigating urban heat island effect: an example from Addis Ababa *Landsc. Urban Plan.* **123** 87–95

Gao K, Santamouris M and Feng J 2020 On the cooling potential of irrigation to mitigate urban heat island *Sci. Total Environ.* **740** 139754

Gillner S, Vogt J, Tharang A, Dettmann S and Roloff A 2015 Role of street trees in mitigating effects of heat and drought at highly sealed urban sites *Landsc. Urban Plan.* **143** 33–42

Hardin P J and Jensen R R 2007 The effect of urban leaf area on summertime urban surface kinetic temperatures: a Terre Haute case study *Urban For. Urban Greening* **6** 63–72

Heaviside C, Macintyre H and Vardoulakis S 2017 The urban heat island: implications for health in a changing environment *Curr. Environ. Health Rep.* **4** 296–305

Huang L, Li J, Zhao D and Zhu J 2008 A fieldwork study on the diurnal changes of urban microclimate in four types of ground cover and urban heat island of Nanjing, China *Build. Environ.* **43** 7–17

Ibsen P C *et al* 2021 Greater aridity increases the magnitude of urban nighttime vegetation-derived air cooling *Environ. Res. Lett.* **16** 034011

Jung M C, Dyson K and Alberti M 2021 Urban landscape heterogeneity influences the relationship between tree canopy and land surface temperature *Urban For. Urban Greening* **57** 126930

Kong F, Yin H, James P, Hutyra L R and He H S 2014 Effects of spatial pattern of greenspace on urban cooling in a large metropolitan area of eastern China *Landsc. Urban Plan.* **128** 35–47

Logan T M, Zaitchik B, Guikema S and Nisbet A 2020 Night and day: the influence and relative importance of urban characteristics on remotely sensed land surface temperature *Remote Sens. Environ.* **247** 111861

Melaas E K, Friedl M A and Zhu Z 2013 Detecting interannual variation in deciduous broadleaf forest phenology using Landsat TM/ETM+ data *Remote Sens. Environ.* **132** 176–85

National Oceanic and Atmospheric Administration 2021 (available at: https://w2.weather.gov/climate/)

O'Neil-Dunne J, MacFaden S and Royar A 2014 A versatile, production-oriented approach to high-resolution tree-canopy mapping in urban and suburban landscapes using GEOBIA and data fusion *Remote Sens.* **6** 12837–65

Oke T 1982 The energetic basis of the urban heat island *Q. J. R. Meteorol. Soc.* **108** 1–24

Pedersen E J, Miller D L, Simpson G L and Ross N 2019 Hierarchical generalized additive models in ecology: an introduction with mgcv *Peer J.* **7** e6876

Quanz J A, Ulrich S, Fenner D, Holtmann A and Eimermacher J 2018 Micro-scale variability of air temperature within a local climate zone in Berlin, Germany, during summer *Climate* **6** 5

Rahman M A, Stratopoulos L M F, Moser-Reischl A, Zölch T, Häberle K H, Rötzer T, Pretzsch H and Pauleit S 2020 Traits of trees for cooling urban heat islands: a meta-analysis *Build. Environ.* **170** 2019

Roberts D A, Quattrochi D A, Hulley G C, Hook S J and Green R O 2012 Synergies between VSWIR and TIR data for the urban environment: an evaluation of the potential for the Hyperspectral Infrared Imager (HyspIRI) Decadal Survey mission *Remote Sens. Environ.* **117** 83–101

Roxon J, Ulm F J and Pellenq R J M 2020 Urban heat island impact on state residential energy cost and CO_2 emissions in the United States *Urban Clim.* **31** 100546

Santamouris M *et al* 2018 Progress in urban greenery mitigation science—assessment methodologies advanced technologies and impact on cities *J. Civil Eng. Manage.* **24** 638–71

Shandas V, Voelkel J, Williams J and Hoffman J 2019 Integrating satellite and ground measurements for predicting locations of extreme urban heat *Climate* **7** 1–13

Shashua-Bar L, Pearlmutter D and Erell E 2009 The cooling efficiency of urban landscape strategies in a hot dry climate *Landsc. Urban Plan.* **92** 179–86

Shiflett S A, Liang L L, Crum S M, Feyisa G L, Wang J and Jenerette G D 2017 Variation in the urban vegetation, surface temperature, air temperature nexus *Sci. Total Environ.* **579** 495–505

Stewart I D and Oke T R 2012 Local climate zones for urban temperature studies *Bull. Am. Meteorol. Soc.* **93** 1879–900

Trust for Public Land 2011 City park facts (available at: http://cloud.tpl.org/pubs/ccpe-city-park-facts-2011.pdf)

Tucker C J 1979 Red and photographic infrared linear combinations for monitoring vegetation *Remote Sens. Environ.* **8** 127–50

U.S. Census Bureau 2019 Quick facts: district of Columbia (available at: www.census.gov/quickfacts/DC)

Voelkel J and Shandas V 2017 Towards systematic prediction of urban heat islands: grounding measurements, assessing modeling techniques *Climate* **5** 41

Vogt P, Riitters K H, Estreguil C, Kozak J, Wade T G and Wickham J D 2007 Mapping spatial patterns with morphological image processing *Landsc. Ecol.* **22** 171–7

Wang K, Jiang S, Wang J, Zhou C, Wang X and Lee X 2017 Comparing the diurnal and seasonal variabilities of atmospheric and surface urban heat islands based on the Beijing urban meteorological network *J. Geophys. Res.* **122** 2131–54

Wood S 2017 *Generalized Additive Models: An Introduction with R* 2nd edn (Boca Raton, FL: CRC Press)

Yao R, Wang L, Huang X, Niu Z, Liu F and Wang Q 2017 Temporal trends of surface urban heat islands and associated determinants in major Chinese cities *Sci. Total Environ.* **609** 742–54

Yu Q, Ji W, Pu R, Landry S, Acheampong M, O' Neil-Dunne J, Ren Z and Tanim S H 2020a A preliminary exploration of the cooling effect of tree shade in urban landscapes *Int. J. Appl. Earth Observ. Geoinf.* **92** 102161

Yu Z, Yang G, Zuo S, Jørgensen G, Koga M and Vejre H 2020b Critical review on the cooling effect of urban blue-green space: a threshold-size perspective *Urban For. Urban Greening* **49** 126630

Zhou D, Xiao J, Bonafoni S, Berger C, Deilami K, Zhou Y, Frolking S, Yao R, Qiao Z and Sobrino J A 2019 Satellite remote sensing of surface urban heat islands: progress, challenges, and perspectives *Remote Sens.* **11** 1–36

Zipper S C, Schatz J, Singh A, Kucharik C J, Townsend P A and Loheide S P 2016 Urban heat island impacts on plant phenology: intra-urban variability and response to land cover *Environ. Res. Lett.* **11** 054023

Ziter C D, Pedersen E J, Kucharik C J and Turner M G 2019 Scale-dependent interactions between tree canopy cover and impervious surfaces reduce daytime urban heat during summer *Proc. Natl Acad. Sci. USA* **116** 7575–80